Available online at www.sciencedirect.com
SCIENCE DIRECT
Polymer Degradation and Stability 84 (2004) 483–492
Polymer Degradation and Stability
www.elsevier.com/locate/polydegstab

Kinetic analysis of the thermal degradation of polystyrene–montmorillonite nanocomposite

Serge Bourbigot[a,*,1], Jeffrey W. Gilman[a], Charles A. Wilkie[b]

[a]*Fire Science Division, Building and Fire Research Laboratory, National Institute of Standards and Technology, Gaithersburg, MD 20899, USA*
[b]*Department of Chemistry, Marquette University, P.O. Box 1881, Milwaukee, WI 53201, USA*

Received 10 December 2003; accepted 4 January 2004

Abstract

Nanocomposites exhibit a combination of unique properties, such as increased heat distortion temperature, reduced permeability, reduced flammability and improved mechanical properties. In this work, a polystyrene (PS) clay nanocomposite was prepared via bulk polymerization using a novel organically modified montmorillonite (MMT). The organic-modifier is the *N*,*N*-dimethyl-*n*-hexadecyl-(4-vinylbenzyl) ammonium chloride (VB16). The thermal stability of PS–VB16 compared to pure PS is examined in pyrolytic and thermo-oxidative conditions. It is then studied using a kinetic analysis. It is shown that the stability of PS is significantly increased in the presence of clay. The thermal behavior of PS and PS nanocomposite is modeled and simulated. A very good agreement between experimental and simulated curves both in dynamic and isothermal conditions is observed. Using kinetic analysis associated to the reaction to fire of PS nanocomposite simulated in a cone calorimeter, the peak of heat release rate is half that of virgin PS, it is suggested that the clay acts as a char promoter slowing down the degradation and providing a protective barrier to the nanocomposite. The combination of these two effects is an important factor lowering the HRR.

Keywords: Kinetic; Thermal degradation; Nanocomposite; Organo-clay; Polystyrene

1. Introduction

Interest in polymer clay nanocomposite has increased significantly in recent years. The property improvements include improved mechanical properties, improved barrier properties, and lower water absorption and reduced flammability [1–6]. To achieve these properties, mica-type layered silicates, such as montmorillonite (MMT), are generally dispersed at the nanoscale level in the polymer to yield the so-called "nanocomposite". The nanocomposite can be prepared via several routes including in situ polymerization [7–9], bulk polymerization [10], solution blending [11,12] or melt-blending in high shear processing environments (extruder or other molding equipment) [13–16].

Polystyrene (PS) is a commodity polymer that is used in a number of commercial products. In 2001, PS was counted amongst the quantitatively most important thermoplastics, and continues to be ranked in fourth place after polyethylene, polypropylene and polyvinylchloride [17]. The main applications include packaging, extruded sheets and consumer electronics. Improved mechanical properties with weight reduction, decreased vapor permeability and low oxygen diffusion are the main development areas for packaging (foamed and foils packaging). Reduced flammability in the area of electronics is also required. All these properties can be achieved using the "nanocomposite approach". Only PS nanocomposite will be considered in this study. The discussion of the preparation and mechanisms involved is beyond the scope of this paper but the reader may

* Corresponding author. Tel.: +33-3-20-43-48-88; fax: +33-3-20-43-65-84.
E-mail address: serge.bourbigot@ensc-lille.fr (S. Bourbigot).
[1] Guest researcher of GEMTEX/ENSAIT. Present address: Laboratory PERF of Ecole Nationale Supérieure de Chimie de Lille, BP 108, 59652 Villeneuve d'Ascq Cedex, France.

0141-3910/$ - see front matter © 2004 Elsevier Ltd. All rights reserved.
doi:10.1016/j.polymdegradstab.2004.01.006

refer to Refs. [1,14,15] and [18] to find useful information.

In our laboratories, we are interested in polymeric materials exhibiting enhanced thermal stability and low flammability. We have shown that polymer nanocomposites meet these requirements at low clay loading, typically between 2 and 5 wt.% [5,10,19,20]. In the pursuit of our efforts for preparing polymer nanocomposite exhibiting such properties, PS nanocomposites were prepared via bulk polymerization using a novel organo-modified MMT clay synthesized by Wilkie and coworkers [10,18]. The organo-modifier is the *N*,*N*-dimethyl-*n*-hexadecyl-(4-vinylbenzyl) ammonium chloride, hereafter called VB16. The flammability of PS nanocomposite containing VB16 clay [18] with clay loading as low as 3 wt.% has been evaluated using the cone calorimeter as fire model [21]. It was found in a previous study that PS–VB16 has a lower heat release rate (HRR) than does the virgin polymer (Fig. 1). The peak of HRR (PHRR) of the virgin PS is 1025 kW/m^2 and that of PS–VB16 nanocomposite falls at 520 kW/m^2. The suggested mechanism by which clay nanocomposites function involves the formation of a char that serves as a barrier to both mass and energy transport.

The fire behavior of a material depends on processes occurring in both condensed and gas phase. These processes strongly depend on the degradation reactions occurring in the condensed phase. So, it is of interest to examine the thermal degradation of polymer clay nanocomposite. In addition to this, it was reported that PS nanocomposites exhibit enhanced thermal stability [18]. Typically, the temperature of degradation is increased.

The kinetics of degradation of polymer nanocomposite is also a major concern in the case of polymer with low flammability such as nanocomposites. So, the kinetic analysis of the nanocomposite, PS–VB16, will be compared to virgin PS. The detailed mechanisms of the degradation reactions of polymers or polymer nanocomposites are generally unknown and in such cases, kinetic analysis of the reaction in the physical–chemical sense is not possible. When an apparatus such as TGA is used for a kinetic study of a degradation process, in fact the rate of evaporation of degradation products is measured, but not the intrinsic chemical reaction (the breaking of bonds) rate. Not every broken bond in the polymer chain leads to the evaporation of product; only polymer chain fragments small enough to evaporate at the given reaction temperature will actually leave the polymer sample. This implies that both physical and chemical processes influence the measured rate of change of the polymer mass and hence the observed pyrolysis or thermo-oxidation kinetics. That is why we will consider in the following that the overall process of degradation of PS and PS–VB16 is described by multistep processes with constant activation energies as suggested by Opfermann [22] and discussed by Mamleev et al. [23,24]. The single steps can be independent, parallel, competitive or consecutive. In other words, an interpretation of these single steps and of their parameters should be done very cautiously.

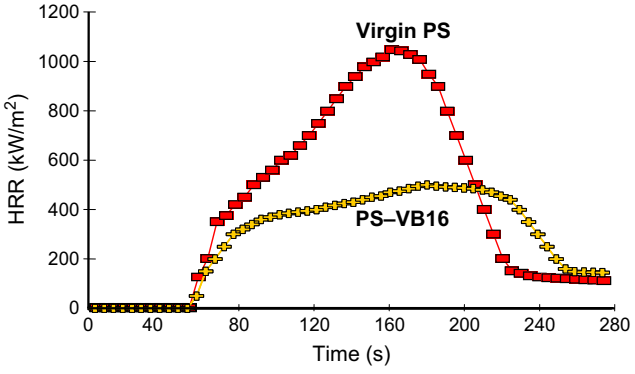

Fig. 1. Heat release rate (HRR) curves versus time of virgin PS and PS–VB16 nanocomposites (external heat flux = 35 kW/m^2).

In this study, thermal stability of PS–VB16 nanocomposite will be examined under different atmospheres and will be considered using a kinetic approach in order to get information on the mode of action of clay in the nanocomposite. TGA curves will be then modeled and the thermal behavior of the polymers will be simulated. Finally, the results of the kinetic analysis are discussed in relation with the flammability properties of the nanocomposite.

2. Experimental[2]

2.1. Preparation of the nanocomposites

The preparation of the nanocomposites used in this study has been described previously, and a general description will only be given here. MMT originated from Southern Clay Products, Inc. (Gonzales, TX, USA). The modified MMT used a sodium-MMT (Cloisite Na^+) as a precursor.

The preparation of the clay (Fig. 2) used in this study, namely, *N*,*N*-dimethyl-*n*-hexadecyl-(4-vinylbenzyl) ammonium chloride, VB16, has been described previously [18]. The preparation of the VB16 nanocomposite with styrene was accomplished by the bulk polymerization

[2] This work was carried out by the National Institute of Standards and Technology (NIST), an agency of the U.S. government and by statute is not subject to copyright in the United States. Certain commercial equipment, instruments, materials or companies are identified in this paper in order to adequately specify the experimental procedure. This in no way implies endorsement or recommendation by NIST. The policy of NIST is to use metric units of measurement in all its publications, and to provide statements of uncertainty for all original measurements. In this document however, data from organizations outside NIST are shown, which may include measurements in non metric units or measurements without uncertainty statements.

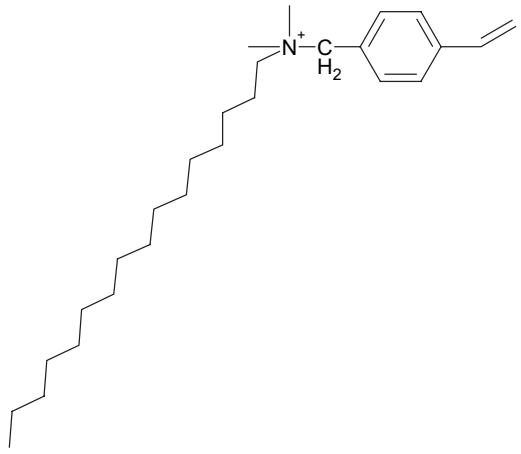

Fig. 2. Structures of the salts used to prepare the organically modified clay VB16.

technique and is described in Ref. [10]. The concentration of the organo-modified (OM) MMT in PS is about 3 wt.%.[3]

2.2. Thermogravimetric and kinetic analysis

Thermogravimetric analysis (TGA) was carried out using a TA Instruments Simultaneous TGA-DTA (SDT 2960) at five heating rates (0.25, 1, 2.5, 5, 15 °C/min) from 25 to 800 °C in air and nitrogen flow (100 cm^3/min). Samples (PS and PS–VB16) of exactly 10 mg (± 0.3 mg) were put in open alumina pans. Typically, three replicates were run for each sample (two for samples run at 0.25 °C/min), and the average was reported. Both the onset (5% mass fraction loss) and peak mass loss rate have an uncertainty of 1.2 °C (2σ). We verified for each heating rate and for each atmosphere that the buoyancy force was negligible. Kinetic analysis and modeling of the degradation of the samples were made using an advanced thermokinetic software package developed by Netzsch Company. The principle has been discussed by Opfermann in Ref. [22] and here we only briefly remind the reader of the basic concepts of the method. For kinetic analysis, it is assumed that the material decomposes according to Eq. (1):

$$A_{solid} \rightarrow B_{solid\ or\ liquid} + C_{gas} \quad (1)$$

The rate expression de/dt, where e is the concentration of educt (reactant), is assumed to be defined by Eq. (2):

$$de/dt = k(T) \times f(e,p) \quad (2)$$

where k is the kinetic constant, p is the concentration of the product, $k = A\exp(-E/RT)$ according to the Arrhenius law, A is the frequency factor, E is the activation energy and $f(e,p)$ is the so-called "reaction equation" or in the case of TGA, the "degradation function".

All reactions are assumed to be irreversible. In the case of degradation and since the evolved gases are continuously removed by the fluid flow in the TGA chamber, this is a reasonable assumption. It is also assumed that the overall reaction (Eq. (1)) is the sum of individual reaction steps (formal or true step) with constant activation energy, as generally accepted in chemistry. The model can then include competitive, independent and successive reactions. The equations are solved with multivariate kinetic analysis (determination of the parameter via a hybrid regularized Gauss–Newton method or Marquardt method) [25].

3. Results and discussion

3.1. Thermal stability of PS and PS–VB16

The TGA curves of the nanocomposite PS–VB16 along with those of virgin PS in pyrolytic and thermo-oxidative conditions are presented in Fig. 3. A small weight loss (around 1.5 wt.%) is observed at about 200 °C, whatever the atmosphere, which can be assigned to the degradation of the organo-modifier of the clay [18]. Under pyrolytic conditions, the thermal stability of the nanocomposite PS–VB16 is enhanced relative to that of virgin polystyrene. The onset temperature of the degradation is about 50 °C higher for the nanocomposites than for the virgin polystyrene. Under thermo-oxidative conditions, the onset temperature of degradation is not significantly enhanced but the charring is dramatically increased (from 6 to 15 wt.% at 400 °C). The char degrades at temperatures higher than 500 °C. The final residues of PS–VB16 observed in the two degradation conditions (about 2 wt.%) can be assigned to the mineral residue of the OM-clay. Oxygen also plays a role in the degradation of PS and PS–VB16.

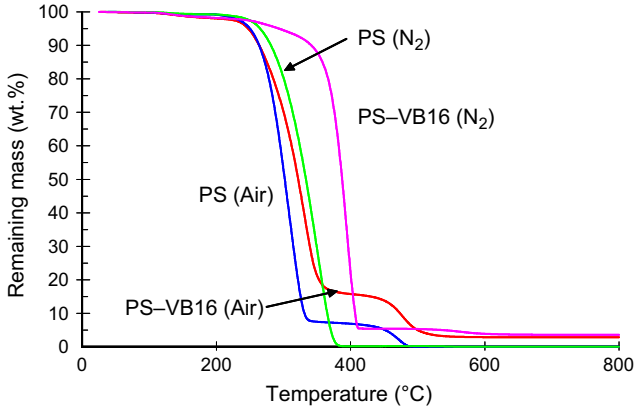

Fig. 3. TG curves of PS and PS–VB16 in pyrolytic and thermo-oxidative conditions (heating rate = 1 °C/min).

[3] wt.% is used in this manuscript and is identical to mass fraction %.

The onset temperature of the main degradation is increased in nitrogen compared to air by 30 °C for virgin PS (from 270 to 300 °C) and by 100 °C for PS–VB16 (from 270 to 370 °C). Enhanced residues in air are also observed in the temperature range of 380–480 °C suggesting that oxygen reacts with PS and/or its degradation products to yield char. The role of oxygen has already been observed [26] and has been fully discussed by Flynn in the case of the degradation of polymers [27]. Oxygen initiates depolymerization leading to the formation of hydroperoxides which can yield char. This char is later degraded at high temperatures. So, reaction of oxygen with the polymeric matrix initiates earlier degradation of the material and then, yielding more char, stabilizes it in a particular temperature range. In the case of nanocomposite, our results suggest that the role of clay is to promote char (transient char) during the thermo-oxidative degradation of the material.

3.2. Kinetic analysis of virgin PS

The degradation of virgin PS under pyrolytic conditions and as a function of the heating rate is presented in Fig. 4. No residue is observed whatever the heating rate is and the shape of the curves and of their derivatives (not shown) might suggest a pyrolytic degradation of PS in one-step reaction, but the evolution of the shape of the curves (the global shape of the curves changes as a function of the heating rate) versus heating rate is an indication of complex reactions.

Before starting any fitting procedure to model the degradation of PS, it is necessary to define a model (combination of reactions) and to preset starting values for the kinetic parameters. Generally, this model is unknown, even if the literature might give some clues for the degradation of PS to start the fit. A convenient approach is to use model-free analysis as a preliminary step of the kinetic analysis [28,29]. A model-free analysis, such as the well-known Friedman analysis, [30] provides the plot of the activation energy versus the fractional weight loss (Fig. 5). This analysis reveals that the activation energy is not constant, but increases from 80 to 180 kJ/mol. This indicates that the degradation does not take place as a one-step reaction but as multi-step reactions, probably as competitive reactions.

According to the previous analysis, the degradation of virgin PS in pyrolytic conditions is modeled using two competitive reactions with Avrami–Erofeev functions (they describe an n-dimensional nucleation/nucleus growth according to Avrami–Erofeev [31]; $f(e) = ne(-\ln(e))^{(n-1)/n}$) giving no residue (B) from A (PS) (Fig. 6). Our model fits the experimental TGA curves very well and the associated kinetic parameters are presented in Table 1. It should be emphasized that our model has a formal character, but no information on the chemistry can be obtained from TGA data only. The true reactions of the system are too complex to be characterized in any fundamental way, so the reactions

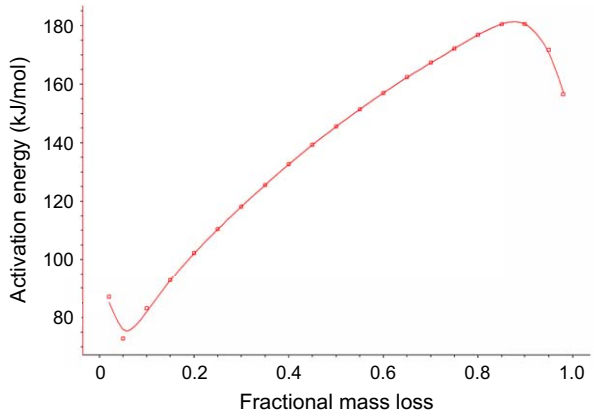

Fig. 5. Activation energies of pure PS versus fractional mass loss determined using the Friedman analysis (N_2 flow).

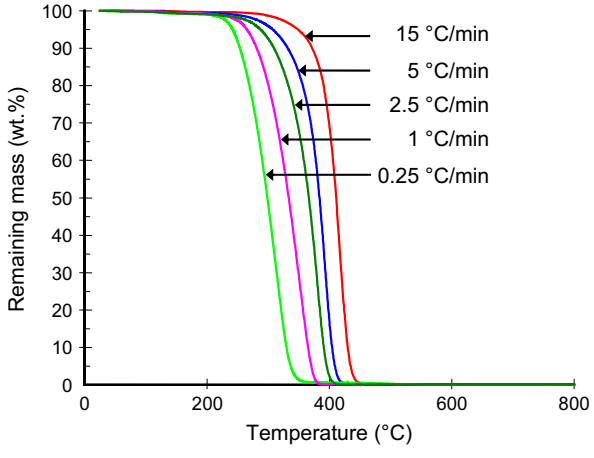

Fig. 4. TG curves of pure polystyrene versus heating rate (N_2 flow).

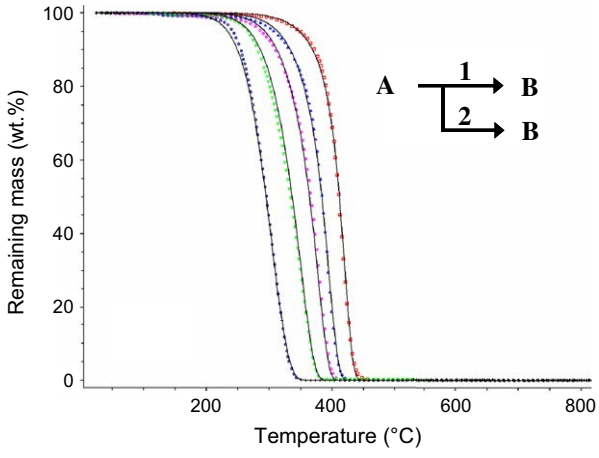

Fig. 6. Experimental (dots) and simulated (line) TG curves of pure polystyrene (N_2 flow).

Table 1
Computed kinetic parameters of the pyrolytic degradation of pure polystyrene

Reaction no.	log(A) (A: s^{-1})	E (kJ/mol)	Dimension
1	14.5 ± 0.1	221.8 ± 4	2.36 ± 0.05
2	3.81 ± 0.04	84.8 ± 0.9	1.09 ± 0.04

are described as pseudo (or lumped) species which are themselves complex materials or a mixture. Among the classical types of global kinetic models, Avrami–Erofeev and n-th order functions are often used to describe the degradation of polymer [32]. Here, the Avrami–Erofeev function was chosen because it gave the highest quality of fit.

Using a global kinetic analysis, Burnham and Braun [32] also suggested a model having two pathways for the pyrolytic degradation because of the changes of PS decomposition reaction profile versus heating rate. Nevertheless, they used only a one-step model in their approach. They found an activation energy of about 255 kJ/mol, which is close to the activation energy determined by our model for reaction 1 (Table 1). Using a one-step model, Peterson et al. found an activation energy of 200 kJ/mol [33]. These two values are consistent with the activation energy we found for reaction 1.

The pyrolysis of PS produces mainly styrene monomer and some oligomers of styrene (dimer, trimer, tetramer and pentamer) [34]. The proposed mechanism is thermal scission of the polymer chain which yields primary radical species. Oligomers are produced via intramolecular radical transfer reaction. Recently, Kruse et al. [35] used a mechanistic model consisting of over 2700 reactions to define the pyrolysis of PS. They confirmed that chain scission (chain fission and chain fission allyl) occurs during the pyrolysis of PS with activation energies between 235 and 280 kJ/mol. Using a bubbling reactor for the pyrolysis of PS, Cha et al. [36] determined the activation energy and the frequency factor of chain scission to be 215 kJ/mol and 9×10^{-13} s^{-1}, respectively. These two approaches did not involve TGA experiments and provide similar data. This is in agreement with the data of reaction 1 of our model (see Table 1). This reaction can then be assigned to the random scission of the polymeric chains. The other reactions involved in the pyrolysis of PS are end-chain and mid-chain β-scission, radical recombination and hydrogen transfer. All these reactions have relatively low activation energies (between 40 and 120 kJ/mol) [34]. Reaction 2 of our model can be assigned to those reactions.

The discussion above shows that we have found kinetic parameters making physical sense. A goal of kinetic analysis is also to simulate the thermal behavior/degradation of a material. If our assumptions are

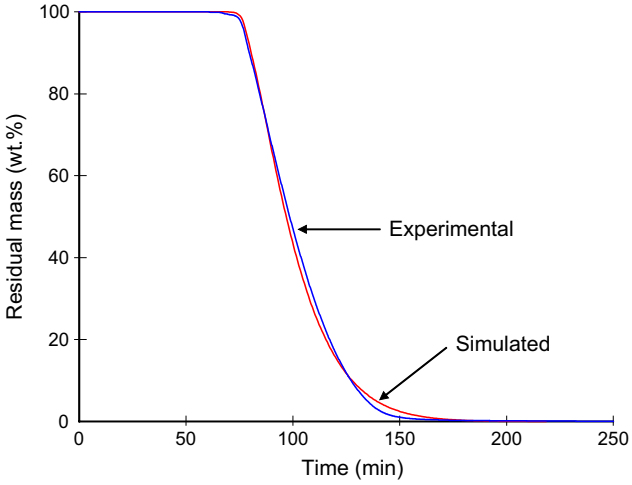

Fig. 7. Experimental and simulated degradation curves of pure PS at 350 °C for 250 min (N_2 flow).

accurate, we should be able to simulate the degradation of PS in isothermal conditions far from the dynamic conditions used to make our modeling. Thus, to verify the accuracy of our model, the degradation of PS was simulated in pyrolytic conditions described as follows:

- isothermal at 25 °C for 60 min (purge of the furnace),
- ramp from 25 to 350 °C at 20 °C/min,
- isothermal at 350 °C for 250 min.

As it is observed in Fig. 7, the simulated curves are in very good agreement with the experimental curves. This means that our approach can be used to model the thermal behavior and the pyrolytic degradation of PS.

As was shown in the previous section, the atmosphere plays a very important role in the degradation of PS. Under thermo-oxidative conditions, the degradation of virgin PS occurs in two main steps (Fig. 8). An intermediate char is formed in the temperature range

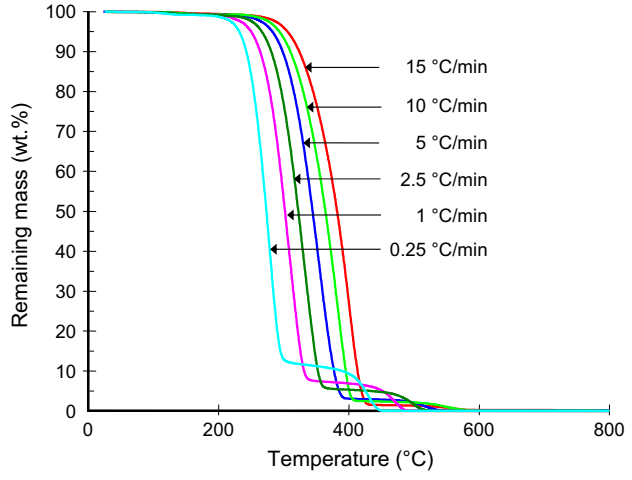

Fig. 8. TG curves of pure polystyrene versus heating rate (air flow).

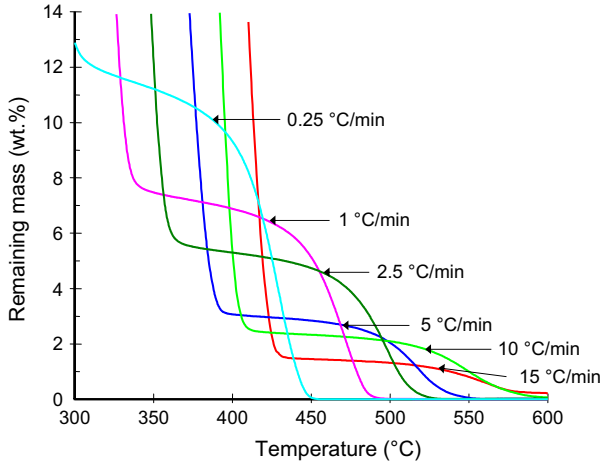

Fig. 9. TG curves of pure polystyrene versus heating rate in the temperature range where the char degrades (air flow). It can be clearly seen that the char yield is dependent on the heating rate.

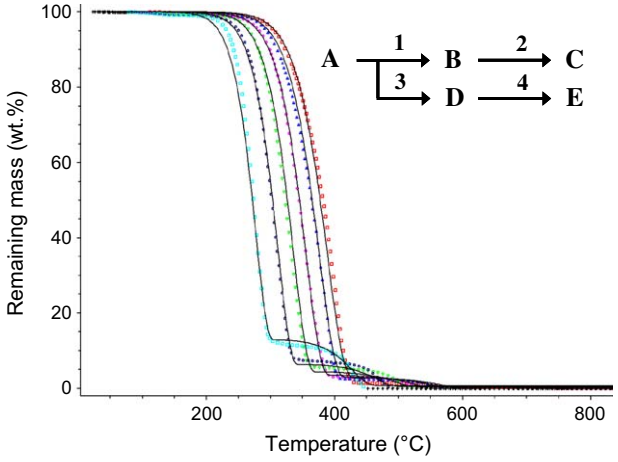

Fig. 11. Experimental (dots) and simulated (line) TG curves of pure polystyrene (air flow).

of 300–550 °C, which is then degraded at higher temperatures. The final residue is zero whatever be the heating rate. In Fig. 9, it can be observed that the char yield formed after the first step of degradation is strongly dependent on the heating rate. This is an evidence of competitive reactions, as confirmed by Friedman analysis (Fig. 10), which shows that the activation energy lies between 85 and 120 kJ/mol ($0.05 <$ fractional mass loss < 0.85) and this non-constancy of activation energy supports the notion of complex reactions. When the fractional mass loss is higher than 0.85, the activation energy becomes unstable, which also supports the idea that the degradation of PS occurs via multi-step reactions.

The degradation of virgin PS under thermo-oxidative conditions is modeled using two sets of two competitive reactions in two successive reactions using pseudo n-th order functions ($f(e)=e^n$) (Fig. 11). These functions provide a much better fit than Avrami–Erofeev functions. Polymer A yields an intermediate complex residue (B and D) via two competitive reactions, these latter materials (B and D) are then degraded into C and E (final residue). This model provides a high quality of fit of the experimental TG curves (Fig. 11). The associated kinetic parameters are presented in Table 2.

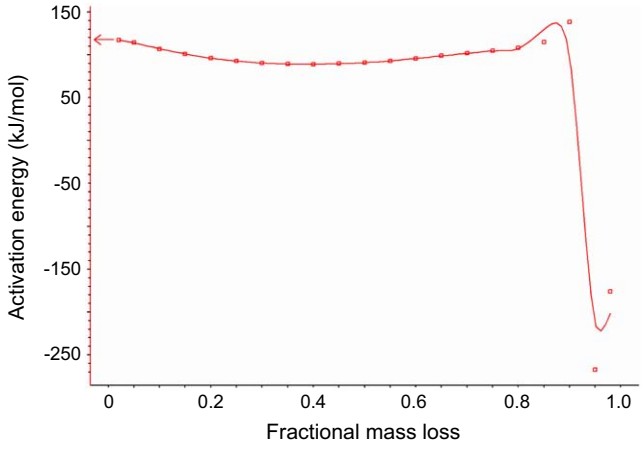

Fig. 10. Activation energies of pure PS versus fractional mass loss determined using the Friedman analysis (air flow).

Thermo-oxidative degradation of polymers involves hydroperoxide radical in the propagation step of degradation. Oxygen initiated depolymerizations have activation energies in the 80–110 kJ/mol range [33]. This supports the value calculated for reaction 1 of the thermo-oxidative degradation of PS. Reaction 3 could be assigned to the molecular decomposition of hydroperoxides. It was shown that this latter reaction is the rate limiting step in the overall kinetics of thermo-oxidative degradation of polymers. The activation energy of this reaction is about 30 kJ/mol and is close to the value of 23.6 kJ/mol suggested by our model. The low heating rate, 0.25 °C/min, used in this study has enabled the determination of the activation energy of reaction 3 with higher precision, i.e., the accuracy of the fit is enhanced. Reactions 2 and 4 of our model can be assigned to char oxidation reactions. The values of activation energies found for the two reactions (122 and 132 kJ/mol) are similar and suggest that char oxidation occurs mainly via one global step process. It is noteworthy that the values are in agreement with global

Table 2
Computed kinetic parameters of the thermo-oxidative degradation of pure polystyrene

Reaction no.	$\log(A)$ (A: s^{-1})	E (kJ/mol)	Reaction order
1	5.89 ± 0.06	102.0 ± 1	0.70 ± 0.02
2	5.90 ± 0.06	131.8 ± 2	0.24 ± 0.01
3	−2.76 ± 0.04	23.6 ± 0.4	2.70 ± 0.05
4	4.98 ± 0.05	122.1 ± 2	0.73 ± 0.02

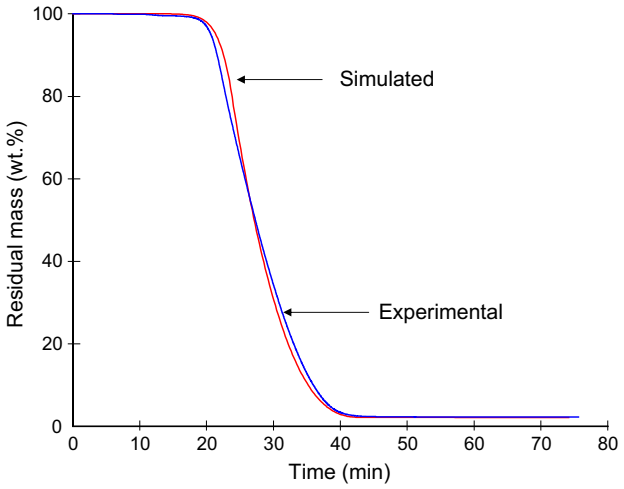

Fig. 12. Experimental and simulated degradation curves of pure PS at 350 °C for 60 min (air flow).

activation energy of char oxidation determined by Kashiwagi and Nambu in the case of the char degradation of cellulosic paper [37].

We verify the accuracy of our modeling by simulating the degradation of PS in thermo-oxidative conditions as follows:

- isothermal at 25 °C for 5 min,
- ramp from 25 to 350 °C at 20 °C/min,
- isothermal at 350 °C for 250 min.

Fig. 12 compares the experimental and the simulated curves and it can be observed that our model can very well predict the thermo-oxidative degradation of PS in isothermal conditions.

3.3. Kinetic analysis of PS clay nanocomposite

In order to study the effects of VB16 on the degradation of PS, PS–VB16 nanocomposite has been investigated in both thermo-oxidative and pyrolytic conditions. TGA curves versus heating rate of PS–VB16 are presented in pyrolytic conditions in Fig. 13 and in thermo-oxidative conditions in Fig. 14. Compared to the pyrolytic degradation of pure PS, PS–VB16 yields an intermediate residue of 4 wt.% in the temperature range of 400–600 °C (compare Fig. 13 against Fig. 4). This residue degrades to yield 2.5 wt.% of final residue. The thermo-oxidative degradation of PS–VB16 occurs in two main steps, like that of the pure PS. The intermediate char is formed in the temperature range of 300–550 °C; it is then degraded at higher temperatures to yield 2.5 wt.% stable char at 800 °C. As in the case of degradation of pure PS, we have evidence of competitive reactions, since the intermediate char yield strongly depends on the heating rate (from 25 wt.% at 0.25 °C/min to 6 wt.% at 15 °C/min) (Fig. 15).

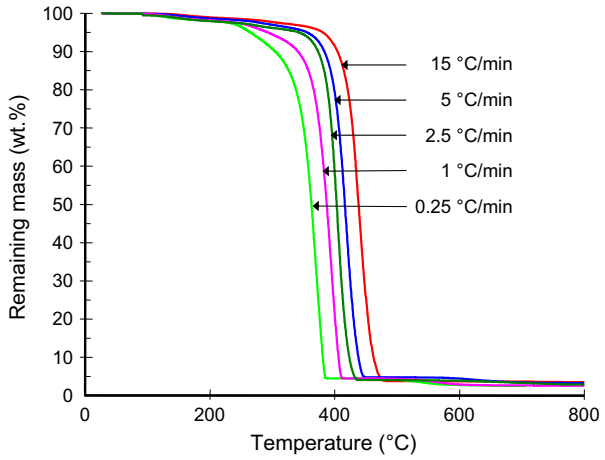

Fig. 13. TG curves of PS–VB16 versus heating rate (N_2 flow).

Using the same approach we did in the previous section, Friedman analysis (curve not shown) shows that activation energy of PS–VB16 in pyrolytic conditions climbs from 80 to 200 kJ/mol and then remains constant ($0.4 <$ fractional mass loss < 0.9). The final part of the curve is chaotic; the activation energy varies from 160 to 240 kJ/mol. This indicates that the degradation occurs via complex reactions and supports the idea of competitive reaction. In the case of thermo-oxidative conditions, the evolution of activation energy according to the Friedman analysis (curve not shown) is constant at 100 kJ/mol up to 0.7 in fractional mass loss and becomes chaotic after that (the activation energy jumps from 150 to −150 kJ/mol). It also supports the fact that the degradation occurs via complex reactions.

According to the conclusions of the Friedman analysis, the degradations of PS–VB16 in pyrolytic (Fig. 16) and in thermo-oxidative (Fig. 17) conditions are modeled using two successive reactions of two competitive reactions with Avrami–Erofeev and *n*-th

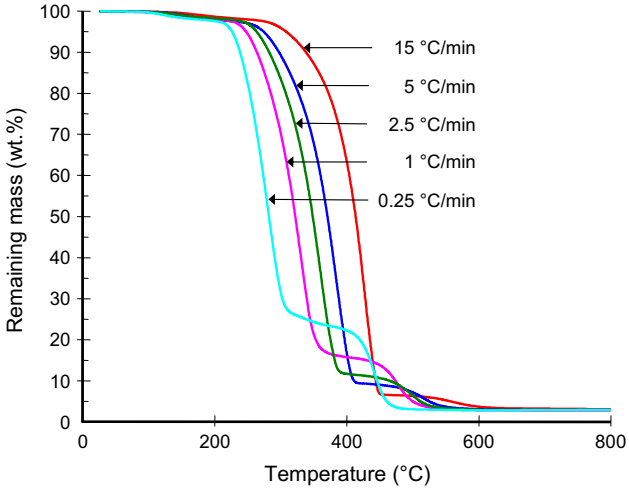

Fig. 14. TG curves of PS–VB16 versus heating rate (air flow).

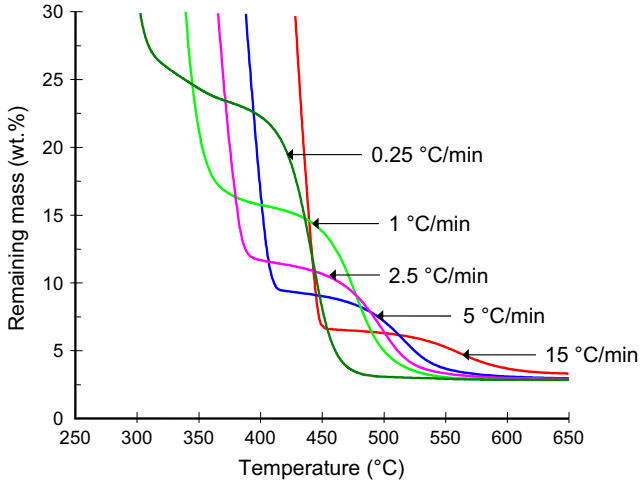

Fig. 15. TG curves of PS–VB16 versus heating rate in the temperature range where the char degrades (air flow). It can be clearly seen that the char yield is dependent on the heating rate.

order functions, respectively. Our models fit well the two sets of curves. The associated kinetic parameters are given in Table 3.

Additional reactions (reactions 2 and 4) have been added to the model to describe the pyrolytic degradation of PS–VB16. During the first degradation step, PS–VB16 exhibits kinetic parameters close to those of pure PS. Nevertheless, the significant difference between the two frequency factors of reaction 3 could explain the enhancement of the thermal stability of PS–VB16 (Fig. 3), suggesting that the probability of end-chain and mid-chain β-scission, radical recombination and hydrogen transfer reactions might be decreased in PS–VB16 nanocomposite.

In the case of the thermo-oxidative degradations, the same reaction schemes have been used for both pure PS and PS–VB16. The computed activation energies of

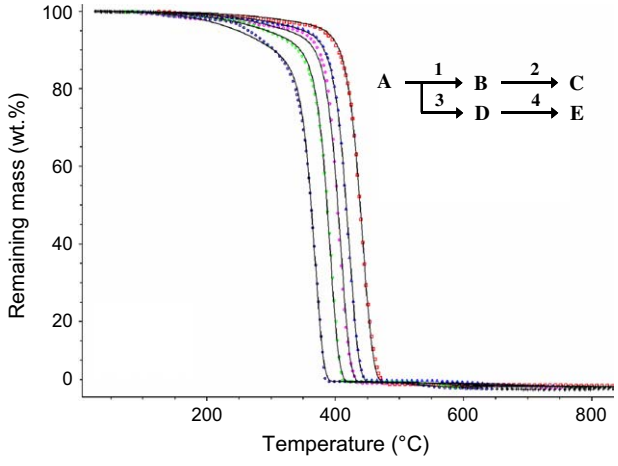

Fig. 16. Experimental (dots) and simulated (line) TG curves of PS–VB16 (N_2 flow).

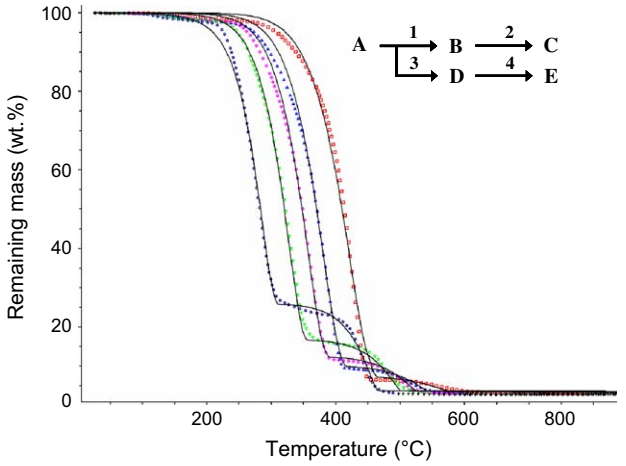

Fig. 17. Experimental (dots) and simulated (line) TG curves of PS–VB16 (air flow).

PS–VB16 are lower than those of PS, except for reaction 3. We propose the following interpretation.

- Reaction 1: oxygen initiated depolymerization of PS. The presence of the clay in PS lowers the energy of this reaction.
- Reaction 3: in competition with reaction 1. The higher activation energy and higher char weights of PS–VB16 suggest that the clay plays the role of char promoter. When measuring at 0.25 °C/min and at 400 °C, the char yield is 10 wt.% for pure PS and 25 wt.% for PS–VB16; the clay content is only 2.5 wt.%.
- Reactions 2 and 4: correspond to char oxidation. The activation energies of reactions 2 and 4 of PS–VB16 compared to pure PS are similar suggesting the same type of reaction of oxidation.

The degradation of PS–VB16 can also be simulated in the conditions of the last section (ramp at 20 °C/min and isothermal at 350 °C) in order to compare the thermal stability of PS–VB16 against pure PS (Fig. 18).

Table 3
Computed kinetic parameters of the thermo-oxidative and pyrolytic degradation of pure polystyrene

Thermo-oxidation			
Reaction no.	log(A) (A: s^{-1})	E (kJ/mol)	Reaction order
1	4.44 ± 0.05	89.2 ± 1	0.60 ± 0.02
2	5.10 ± 0.06	124.9 ± 2	1.30 ± 0.01
3	−0.94 ± 0.02	35.3 ± 0.2	2.90 ± 0.05
4	4.18 ± 0.05	118.8 ± 2	0.30 ± 0.01
Pyrolysis			
Reaction no.	log(A) (A: s^{-1})	E (kJ/mol)	Dimension
1	12.4 ± 0.1	196.4 ± 3	1.45 ± 0.04
2	5.68 ± 0.04	144.3 ± 0.9	1.50 ± 0.04
3	−0.15 ± 0.02	67.1 ± 0.3	0.42 ± 0.01
4	3.48 ± 0.04	111.0 ± 1	2.32 ± 0.05

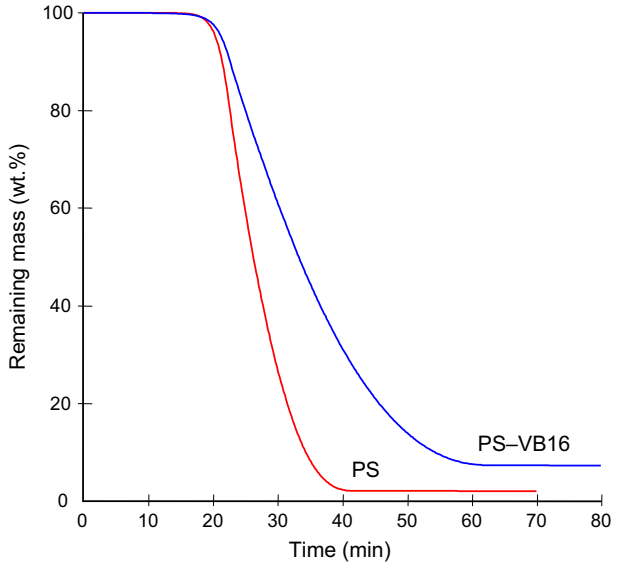

Fig. 18. Simulated curves of the thermo-oxidative degradation of PS and PS–VB16 in isothermal conditions at 350 °C after a ramp of 20 °C/min.

In such conditions the nanocomposite also exhibits better thermal stability than pure PS. The degradation of the two systems starts at the same time but the degradation rate of PS is faster than that of the nanocomposite. The final residues at 80 min are 10 and 3 wt.% for PS–VB16 and PS, respectively.

3.4. Some considerations on kinetic analysis related to flammability of PS clay nanocomposite

Kinetic analysis and heat stability of PS can be related to flame retardancy even if kinetic approach does not take into account heat and mass transfer. To do this, let us assume that the samples exhibit 'thermally thin behavior'. If we consider the fire behavior of samples in a cone calorimeter experiment, materials generally exhibit 'thermally thick behavior' but we can imagine as a first hypothesis that the sample is the superposition of an 'infinite' number of layers of thermally thin material without (or few) interaction between the layers. Our kinetic approach might then provide some information on the behavior of the samples. It is of course, not our goal to describe the complete fire behavior of our samples using kinetic analysis.

Fig. 19 shows the assignment of different sections of the HRR curve of PS–VB16. The first period of time corresponds to the 'heating' of the sample and it can be assumed that the sample undergoes a thermo-oxidative degradation. As shown in Fig. 1, the times to ignition of PS and PS–VB16 are not modified by the presence of the clay. The kinetic analysis has shown that the presence of clay lowers the activation energy of the polymer, but does not increase the onset temperature of degradation (reaction 1 of the model corresponding to the depolymerization of PS initiated by oxygen). It can encourage an easier degradation of the polymer upon heating but, as suggested by the negligible change in onset temperature, it does not lead to an earlier ignition. After the time to ignition, the polymer burns and reaches its maximum HRR. During this time, pyrolysis of the material mainly occurs (consumption of the oxygen). The clay delays chain scission and forms a protective alumino-silica barrier (see Ref. [38] for the discussion on the mechanism of formation of the protective barrier) which leads to the reduction of HRR peak. After reaching HRR peak, a pseudo-steady state is observed (HRR is constant), the sample burns with flames not uniformly distributed at the surface of the material. During this step, we can assume that both thermo-oxidative and pyrolytic degradation occur. The clay barrier causes increased charring, which would be an addition to the efficiency of the barrier. Accordingly, a strong temperature gradient should be observed inside the material, which means that the different 'thermally thin layers' of material undergo different heating rates and that charring reactions can be promoted (reactions with low activation energies, i.e., reaction 3 of the degradation pathway, are favored when heating rate is slow). Nevertheless, the time of combustion of PS–VB16 is longer than that of PS, suggesting that even if a protective barrier is formed at the surface of the material, its efficiency is not enough to stop the

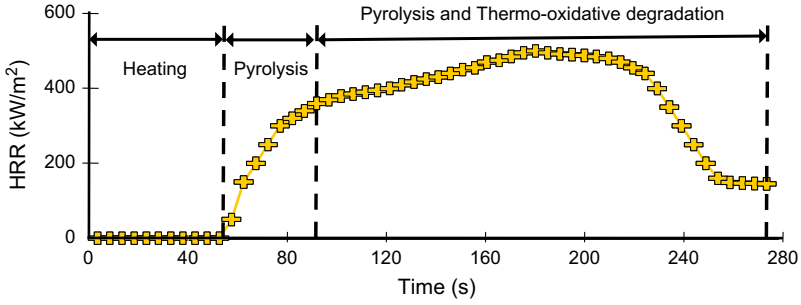

Fig. 19. Assignment of different sections of the HRR curve of PS–VB16 versus time (external heat flux = 35 kW/m^2).

combustion. The 'fuel flow' (evolving degradation gases) feeding the flame is probably slowed down, decreasing and spreading out HRR.

4. Conclusion

The thermal degradation of a PS nanocomposite was studied and described using a kinetic analysis. The thermal stability of PS is significantly increased in the presence of the clay under both pyrolytic and thermo-oxidative conditions. The thermal behavior of PS and PS nanocomposite have been modeled and simulated and we have shown a very good agreement between experimental and simulated curves both in dynamic and isothermal conditions. Using kinetic analysis associated with the reaction to fire of PS nanocomposite simulated in a cone calorimeter, it is suggested that the clay acts a char promoter slowing down the degradation and providing a transient protective barrier to the nanocomposite in combination with the alumino-silica barrier which arises from the clay. The combination of these two effects is an important factor lowering the HRR.

References

[1] Alexandre M, Dubois P. Mater Sci Eng R 2000;28(1–2):1–63.
[2] Kojima Y, Usuki A, Kawasumi M, Okada A, Fukushima Y, Kurauchi T, et al. J Mater Res 1993;8(5):1185–9.
[3] Okada A, Fukushima Y, Kawasumi M, Inagaki S, Usuki A, Sugiyama S, et al. US Patent 4,739,007, 1988.
[4] Messersmith PB, Giannelis EP. J Polym Sci A Polym Chem 1995;33(7):1047–57.
[5] Gilman JW, Kashiwagi T, Lichtenhan JD. SAMPE J 1997; 33:40–6.
[6] Gilman JW. Appl Clay Sci 1999;15(1–2):31–49.
[7] Usuki A, Kojima Y, Kawasumi M, Okada A, Fukushima Y, Kurauchi T, et al. J Mater Res 1993;8:1179–84.
[8] Messersmith PB, Giannelis EP. Chem Mater 1994;6:1719–25.
[9] Wang MS, Pinnavaia TJ. Chem Mater 1994;6:468–74.
[10] Zhu J, Wilkie CA. Polym Int 2000;49:1158–63.
[11] Jeon HG, Jung HT, Lee SD, Hudson S. Polym Bull 1998;41(1):107–13.
[12] Gilman JW, Awad WH, Davis RD, Shields J, Harris RH, Davis C, et al. Chem Mater 2002;14:3776–85.
[13] Giannelis E. Adv Mater 1996;8(1):29–39.
[14] Gilman JW, Kashiwagi T, Giannelis EP, Manias E, Lomakin S, Lichtenhan JD, et al. In: Le Bras M, Camino G, Bourbigot S, Delobel, editors. Fire retardancy of polymers—the use of intumescence. Cambridge: The Royal Society of Chemistry; 1998. p. 223–35.
[15] Gilman JW, Jakson CL, Morgan AB, Harris RH, Manias E, Giannelis EP, et al. Chem Mater 2000;12:1866–73.
[16] Devaux E, Bourbigot S, El Achari A. J Appl Polym Sci 2002;86:2416–23.
[17] Wagner D. Kunstoffe 2002;92(10):17–9.
[18] Zhu J, Morgan AB, Lamelas FJ, Wilkie CA. Chem Mater 2001;13:3774–80.
[19] Bourbigot S, Devaux E, Flambard X. Polym Degrad Stab 2002;75(2):397–402.
[20] Dabrowski F, Bourbigot S, Delobel R, Le Bras M. Eur Polym J 2000;36(2):273–84.
[21] Babrauskas V. Development of cone calorimeter—a bench scale rate of heat release based on oxygen consumption, NBS-IR 82-2611, US Nat Bur Stand, Gaithersburg, 1982.
[22] Opfermann J. J Therm Anal Calorim 2000;60:641–58.
[23] Mamleev V, Bourbigot S. J Therm Anal Calorim 2002;70:565–79.
[24] Mamleev V, Bourbigot S, Le Bras M, Lefevbre J. Submitted for publication.
[25] Kaisersberger E, Opfermann. Thermochim Acta 1991;187:151–8.
[26] Rose N, Le Bras M, Bourbigot S, Delobel R, Costes B. Polym Degrad Stab 1996;53(2–3):355–60.
[27] Flynn JH. Polymer degradation. In: Cheng ZD, editor. Handbook of thermal analysis and calorimetry, vol. 3. Amsterdam: Elsevier; 2002.
[28] Opfermann J, Kaisersberger E, Flammersheim HJ. Thermochim Acta 2002;391:119–27.
[29] Sewry JD, Brown ME. Thermochim Acta 2002;390:217–25.
[30] Friedman HL. J Polym Sci C 1964;6:183–9.
[31] Erofeev BV. CR Dokl Akad Sci USSR 1946;52:511–4.
[32] Burnham AK, Braun RL. Energy Fuels 1999;13(1):1–22.
[33] Peterson JD, Vyazovkin S, Wight CA. Macromol Chem Phys 2001;202:775–84.
[34] Grassie N, Scott G. Polymer degradation and stabilisation. Cambridge: Cambridge University Press; 1985.
[35] Kruse TM, Woo OS, Wong HW, Khan SS, Broadbelt LJ. Macromolecules 2002;35:7830–44.
[36] Cha WS, Kim SB, McCoy BJ. J Korean Chem Eng 2002;19(2):239–45.
[37] Kashiwagi T, Nambu H. Combust Flame 1992;88:345–68.
[38] Wang J, Du J, Zhu J, Wilkie CA. Polym Degrad Stab 2002;77:249–52.